Title

An Accessible Chiral Linker to Enhance Potency and Selectivity of Neuronal Nitric Oxide Synthase Inhibitors.

Journal

ACS Medicinal Chemistry Letters, 5(1)

ISSN

1948-5875

Authors

Jing, Qing

Roman, Linda

Martásek, Pavel

et al.

Publication Date

2014-01-09

DOI

10.1021/ml400381s

Peer reviewed

ACS Medicinal Chemistry Letters

Letter

pubs.acs.org/acsmedchemlett

Accessible Chiral Linker to Enhance Potency and Selectivity of Neuronal Nitric Oxide Synthase Inhibitors

Qing Jing,[†] Huiying Li,[‡] Linda J. Roman,[§] Pavel Martásek,[§,∥] Thomas L. Poulos,*[,‡] and Richard B. Silverman*[,†]

[†]Department of Chemistry, Department of Molecular Biosciences, Chemistry of Life Processes Institute, Center for Molecular Innovation and Drug Discovery, Northwestern University, Evanston, Illinois 60208-3113, United States

[‡]Departments of Molecular Biology and Biochemistry, Pharmaceutical Sciences, and Chemistry, University of California, Irvine, California 92697-3900, United States

[§]Department of Biochemistry, The University of Texas Health Science Center, San Antonio, Texas 78384-7760, United States

[∥]Department of Pediatrics, First Faculty of Medicine, Charles University, Prague, Czech Republic

Supporting Information

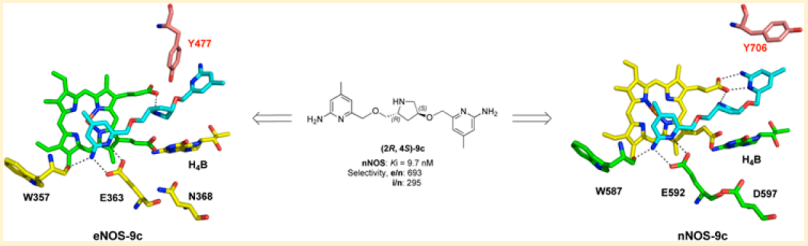

ABSTRACT: The three important mammalian isozymes of nitric oxide synthase (NOS) are neuronal NOS (nNOS), endothelial NOS (eNOS), and inducible NOS (iNOS). Inhibitors of nNOS show promise as treatments for neurodegenerative diseases. Eight easily synthesized compounds containing either one (**20a,b**) or two (**9a−d**; **15a,b**) 2-amino-4-methylpyridine groups with a chiral pyrrolidine linker were designed as selective nNOS inhibitors. Inhibitor **9c** is the best of these compounds, having a potency of 9.7 nM and dual selectivity of 693 and 295 against eNOS and iNOS, respectively. Crystal structures of nNOS complexed with either **9a** or **9c** show a double-headed binding mode, where each 2-aminopyridine headgroup interacts with either a nNOS active site Glu residue or a heme propionate. In addition, the pyrrolidine nitrogen of **9c** contributes additional hydrogen bonds to the heme propionate, resulting in a unique binding orientation. In contrast, the lack of hydrogen bonds from the pyrrolidine of **9a** to the heme propionate allows the inhibitor to adopt two different binding orientations. Both **9a** and **9c** bind to eNOS in a single-headed mode, which is the structural basis for the isozyme selectivity.

KEYWORDS: *Nitric oxide, nitric oxide synthase, enzyme inhibition, neurodegenerative diseases*

Nitric oxide (NO), which is synthesized from L-arginine by the nitric oxide synthase (NOS) family of enzymes, plays many fundamental physiological roles in mammals. Although all three isoforms of NOS, neuronal NOS (nNOS), endothelial NOS (eNOS), and inducible NOS (iNOS), produce NO as an important second messenger molecule, overexpression of NO by nNOS in brain is associated with many neurodegenerative diseases, including Parkinson's,[1] Alzheimer's,[2] Huntington's,[3] migraine headaches,[4] and neuronal damage from stroke.[5] Inhibition of nNOS is a potential treatment for neurodegeneration;[6−8] however, it is challenging to make a selective inhibitor of nNOS over eNOS and iNOS in order to prevent side effects, such as hypertension, and not to interfere with normal immunological functions. The high similarity of NOS isozymes, particularly the heme active site structure, is the reason that most of the reported inhibitors provide limited isozyme selectivity,[9−13] even though those molecules bind at the active site and afford excellent potency. While some highly selective nNOS inhibitors have been successfully developed in our group,[14] the integration of easy synthesis, bioavailability, and selectivity remains a challenge.

We have previously developed two lead compounds (**1** and **2**, Figure 1) that exhibit excellent potency against nNOS. Despite the high selectivity of compound **1**,[15] the tedious synthesis limits its structure/activity optimization to improve bioavailability. The synthesis of **2** is much easier than that of **1**, but its selectivity needs to be improved.[16] Compound **3** features advantages of synthetic ease and good activity for the next generation of inhibitors. In this work, we design a new class of inhibitors, using a straightforward synthesis, having excellent inhibition properties.[17] These compounds, which exhibit unique binding features with NOS, provide a basis for developing this integrative strategy of ease of synthesis and

Received: September 8, 2013
Accepted: November 5, 2013
Published: November 5, 2013

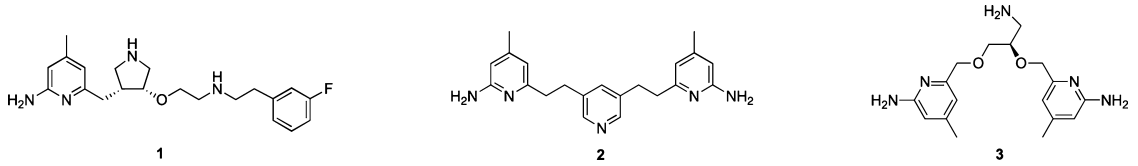

Figure 1. Structures of lead compounds **1**, **2**, and **3**.

inhibitor structure for improved inhibition potency and isozyme selectivity. Because the inhibitors derive from chiral natural scaffolds that are commercially available, there is no need for chiral synthesis or resolution, which makes these new compounds easily accessible and ready for further optimization.

Compounds **9a−d** were synthesized via the route shown in Scheme 1. Starting from the corresponding chiral proline

Scheme 1. Chemical Synthesis of 9a−d[a]

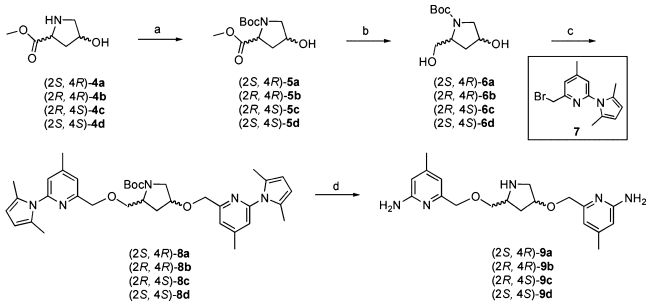

[a]Reagents and conditions: (a) $(Boc)_2O$, CH_3OH, 86−91%. (b) $LiBH_4$, THF, 94−98%. (c) NaH, DMF, compound **7**, 0 °C, 80−86%. (d) (i) NH_2OH−HCl, EtOH/H_2O (2/1); (ii) 2 M HCl in CH_3OH/dioxane (1/1), two steps, 68−81%. Note: The synthesis of **7** follows the literature report.[18]

analogues **4**, the secondary amine was protected as a Boc carbamate in methanol, and then the methyl ester was reduced to an alcohol with $LiBH_4$ in excellent yields. Diol **6** was allowed to react with **7** in the presence of NaH, providing doubly substituted **8** in one step. After deprotection of the amino groups of the 2-aminopyridines with NH_2OH−HCl and the Boc protecting group under acidic conditions, **9** was obtained successfully.

The synthesis of **15** requires two key intermediates, **11** and **12**, as shown in Scheme 2. Starting from **5**, ether formation with **7** afforded **10**, followed by reduction with $LiBH_4$, gave **11**. Under similar conditions, ethylene glycol reacted with **7**, yielding **12**, which was brominated with PPh_3 and CBr_4 in THF to give **13**. Base-promoted reaction of **11** and **13** produced **14**; deprotection gave **15**.

As described in Scheme 3, compound **18**, a key intermediate to **20**, was prepared from 3-fluorophenylmethanol by allylation, oxidation to the aldehyde,[19] reduction to the alcohol, and bromination. Coupling of **18** with **11** gave **19**, which was deprotected, as described above, to generate **20**.

All inhibitors were assayed against three different isoforms of NOS, including rat nNOS, bovine eNOS, and murine macrophage iNOS using L-arginine as a substrate. K_i values and selectivities are summarized in Table 1. The new compounds contain a similar five-membered ring linker as does **1**, which derives from proline analogues. Reference compound **3** can be regarded as having a bioisosteric open-chain pyrrolidine. Four isomers of **9** (**9a−d**) exhibit excellent potency against nNOS, but **9c** is most potent (9.7 nM) and

Scheme 2. Chemical Synthesis of 15a,b[a]

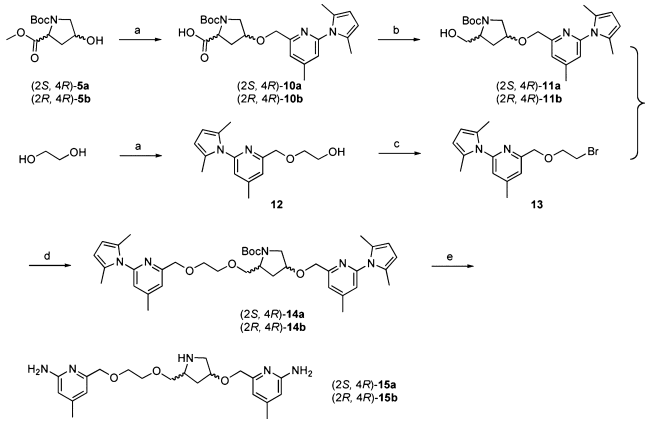

[a]Reagents and conditions: (a) NaH, DMF, **7**, 0 °C, 86−87%. (b) $LiBH_4$, THF, 87−91%. (c) PPh_3, CBr_4, THF, 81%. (d) NaH, DMF, NaI, 0 °C, 45−50%. (e) (i) NH_2OH−HCl, EtOH/H_2O (2/1); (ii) 2 M HCl in CH_3OH/dioxane (1/1), two steps, 70−73%.

Scheme 3. Chemical Synthesis of 20a,b[a]

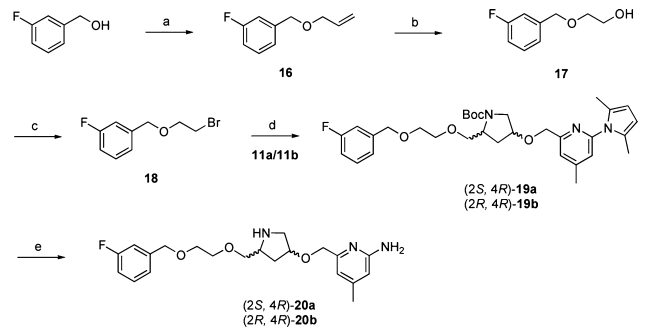

[a]Reagents and conditions: (a) NaH, DMF, allyl bromide, 0 °C, 84%. (b) (i) $RuCl_3$, $NaIO_4$, $BnEt_3NCl$, EtOAc; (ii) TMSCl, $LiBH_4$, two steps, 76%. (c) PPh_3, CBr_4, CH_2Cl_2, 82%. (d) NaH, DMF, NaI, 0 °C, 51−53%. (e) (i) NH_2OH−HCl, EtOH/H_2O (2/1); (ii) 2 M HCl in CH_3OH/dioxane (1/1), two steps, 74−78%.

selective (693- and 295-fold for nNOS over eNOS and iNOS, respectively). We extended the left arm of the (2*S*, 4*R*) and (2*R*, 4*R*) isomer to give **15a,b**. However, both were less potent and selective than **9**. Replacement of one of the 2-amino-4-methylpyridine groups with a 3-fluorophenyl moiety (**20a,b**) decreased the potency further.

Not surprisingly, the stereochemistry of inhibitors significantly affects binding. To understand the structure−activity relationship of these inhibitors, we have determined the crystal structures of **9a** and **9c** complexed with rat nNOS (Figure 2). While the 2-aminopyridine with a 3-atom ether linker to the center pyrrolidine ring hydrogen bonds to Glu592, the 2-aminopyridine with a 2-atom ether linker hydrogen bonds to the heme propionate D. In order for the 2-aminopyridine group to make two hydrogen bonds with the heme propionate D,

dx.doi.org/10.1021/ml400381s | *ACS Med. Chem. Lett.* 2014, 5, 56−60

Table 1. K_i[a] Values of Inhibitors for nNOS, eNOS, and iNOS

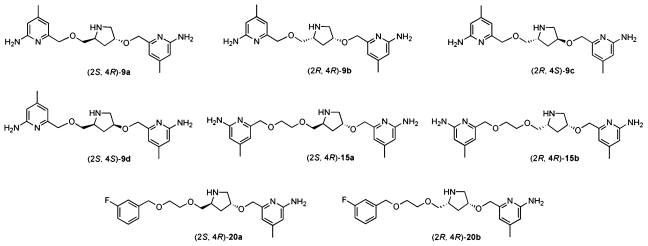

	K_i[a] (nM)			selectivity[b]	
inhibitors	nNOS	eNOS	iNOS	e/n	i/n
9a	26	2179	2271	84	87
9b	34	3473	5588	102	164
9c	9.7	6727	2866	693	295
9d	31	2356	1902	76	61
15a	70	6248	2316	89	33
15b	199	9300	13564	47	68
20a	153	7963	5858	52	38
20b	330	11726	8472	35	26

[a]The IC_{50} values were measured for three different isoforms of NOS, rat nNOS, bovine eNOS, and murine macrophage iNOS, using L-arginine as a substrate with standard deviation of ±10%. The corresponding K_i values were calculated from the IC_{50} values using the equation $K_i = IC_{50}/(1 + [S]/K_m)$ with known K_m values (nNOS, 1.3 μM; iNOS, 8.3 μM; eNOS, 1.7 μM). [b]The ratio of K_i (eNOS or iNOS) to nNOS.

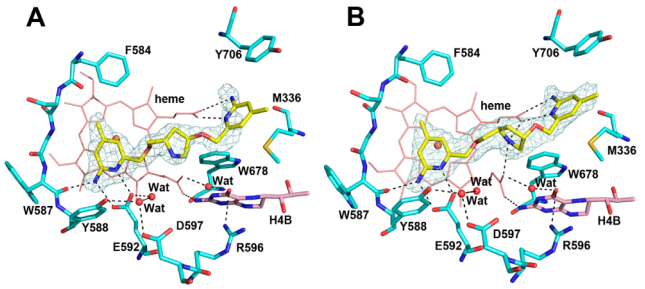

Figure 2. View of the active site of nNOS in complex with inhibitor **9a** (A) and **9c** (B). Shown also are the omit $F_o - F_c$ density maps for inhibitor contoured at the 2.5σ level. Relevant hydrogen bonds are depicted as dashed lines. All structural figures were prepared with PyMol (www.pymol.org).

Trp706, which normally H-bonds to the heme propionate, must move out of the way and adopt a new rotamer conformation. In addition, because of the different chirality, the ring N atom from the center pyrrolidine in **9c** points toward the heme where it can H-bond (2.7−3.0 Å) with both propionates (Figure 2B). In contrast, the pyrrolidine ring N atom in **9a** makes no hydrogen bonds with the heme (Figure 2A). This difference in the pyrrolidine ring orientation results in better binding affinity for **9c** (9.7 nM) compared to that for **9a** (26 nM), which is consistent with the much better electron density quality shown in the crystal structure of former than that of the latter. The lack of hydrogen bonding from the pyrrolidine ring of **9a** to the heme propionates allows a different inhibitor binding orientation in subunit B, where **9a** flips 180°. This places the 2-aminopyridine with a 2-atom ether linker to pyrrolidine in the active site, where it H-bonds with Glu592, as illustrated in Figure S1 (see Supporting Information). Note that the normal binding orientation, as shown in Figure 2A, can coexist with the flipped one as an alternate conformation, but because of the limited data resolution, and for simplicity, only the flipped orientation was modeled into subunit B.

Inspired by compounds **1**−**3**, we designed **15a**,**b** and **20a**,**b**, except without a basic nitrogen atom in the linker, to match a similar size and/or structure of **1**. Unfortunately, none of these compounds afforded improved potency or selectivity. These results suggest that a long ether bonded linker arm in this series of compounds is not a promising strategy.

It is interesting to compare the binding mode differences between the best inhibitor reported here, **9c**, with the lead compounds in Figure 1. The aminopyridine in **1** makes bifurcated H-bonds with the heme propionate D, while the pyrrolidine nitrogen directly H-bonds to both the heme propionate A and H_4B,[15] which affords the inhibitor low nanomolar potency and more than 2500-fold selectivity for nNOS over eNOS. Although the interactions from the aminopyridine to the heme propionate D are preserved with one of the two head groups in **9c**, the longer 2-atom spacer only allows the pyrrolidine nitrogen of **9c** to H-bond with heme propionate A and not with H_4B (Figure 2B). The double-headed binding mode initially observed with lead compound **2**[16] is retained with **9c**. The additional H-bonding interaction introduced by the pyrrolidine nitrogen to the heme makes **9c** a more potent inhibitor than **2**. Being able to establish both double-headed binding, as well as a H-bond from the pyrrolidine N atom to heme in **9c**, provides an improvement compared to **3**, which has lost its H-bonds from the second aminopyridine to the heme propionate D because of the short 2-atom linker between the chiral center and the headgroup.[17]

To interpret the isozyme selectivity reported in Table 1, we also determined the crystal structures of **9a** and **9c** complexed with bovine eNOS. As shown in Figure 3, for both **9a** and **9c**,

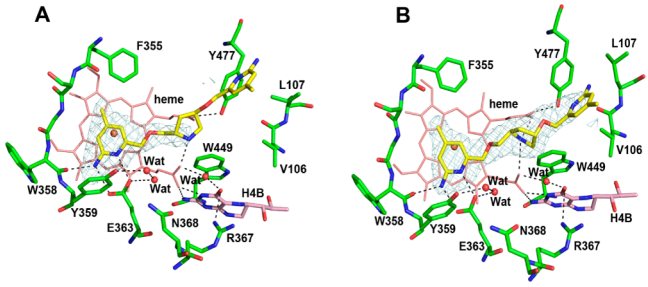

Figure 3. View of the active site of eNOS in complex with inhibitor **9a** (A) and **9c** (B). Shown also are the omit $F_o - F_c$ density maps for the inhibitors contoured at the 2.5σ level. Relevant hydrogen bonds are depicted as dashed lines.

only a single 2-aminopyridine, the one with a 3-atom ether linker to the pyrrolidine, makes hydrogen bonds with Glu363. The other 2-aminopyridines cannot interact with the heme propionate D because Tyr477 is still in position to hydrogen bond with the same propionate. As a result, the second 2-aminopyridine is disordered in both eNOS structures. The disordering is more severe for **9a** than for **9c**, possibly because the hydrogen bonding geometry between the pyrrolidine and the heme propionates is much poorer in the former (Figure 3A) than that seen in the latter (Figure 3B). The exact position of the second 2-aminopyridine in **9a** is poorly defined.

On the basis of what we know about the binding features of **9a** and **9c** to nNOS and eNOS, we expect that compounds

dx.doi.org/10.1021/ml400381s | ACS Med. Chem. Lett. 2014, 5, 56−60

15a,b and **20a,b** can still bind to NOS through hydrogen bonds from the active site Glu to the 2-aminopyridine with a 2-atom ether linker to the pyrrolidine. This would allow the pyrrolidine ring N atom to interact with the heme propionate(s). However, the extended ether linkers to the second 2-aminopyridine (**15a,b**) or to the fluorophenyl moiety (**20a,b**), most likely, result in steric clashes between the long tail of the inhibitors and the surrounding protein, which is reflected in their poor affinity to both nNOS and eNOS (Table 1).

The binding of **9a** and **9c** to nNOS and eNOS teaches us again the importance of inhibitor chirality and NOS active site dynamics. We have a number of examples of double-headed aminopyridine inhibitors that bind to nNOS in multiple orientations but to eNOS only in a single orientation.[20] The conserved Tyr residue (Tyr706 in nNOS or Tyr477 in eNOS) that normally hydrogen bonds to heme propionate D can adopt a different rotamer conformation, leaving space for the aminopyridine of the inhibitor to make hydrogen bonds to the heme propionate. This difference between nNOS and eNOS results from the ability of Tyr706 to more readily adopt alternate rotamer conformations than can Tyr477 in eNOS. This enhanced dynamics and adaptability of nNOS is no doubt an important structural basis that we can utilize in designing isozyme selective NOS inhibitors.

In conclusion, we have designed and synthesized double-headed compounds with a chiral linker derived from proline, which has substantially simplified the synthesis of these inhibitors relative to that for **1** and increased selectivity relative to **2**. Inhibitor (2*R*, 4*S*)-**9c** affords excellent potency (9.7 nM) as well as dual selectivity (693- and 295-fold for nNOS over eNOS and iNOS, respectively). With the application of our integrative strategy, easy accessibility and good inhibitory properties are taken into account during inhibitor design. Combined with our earlier work on double-headed inhibitors, we not only developed a series of potent and selective inhibitors but also provided an efficient methodology for the design of small molecules and accelerated the structure optimization process.

■ ASSOCIATED CONTENT

Supporting Information

Synthetic procedures, characterization of compounds, including ^{1}H and ^{13}C NMR spectra, assay details, and crystallographic procedures. This material is available free of charge via the Internet at http://pubs.acs.org.

■ AUTHOR INFORMATION

Corresponding Authors

*(R.B.S.) E-mail: agman@chem.northwestern.edu. Tel: +1-847-491-5653.

*(T.L.P.) E-mail: poulos@uci.edu. Tel: +1-949-824-7020.

Author Contributions

The manuscript was written through contributions of all authors. All authors have given approval to the final version of the manuscript.

Notes

The authors declare no competing financial interest.

■ ACKNOWLEDGMENTS

We are grateful for financial support from the National Institutes of Health (GM049725 to R.B.S. and GM057353 to T.L.P.). We thank Dr. Bettie Sue Siler Masters (NIH grant GM52419, with whose laboratory P.M. and L.J.R. are affiliated). B.S.S.M. also acknowledges the Welch Foundation for a Robert A. Welch Distinguished Professorship in Chemistry (AQ0012). P.M. is supported by grant 0021620849 from MSMT of the Czech Republic. We thank the beamline staff at SSRL and ALS for their assistance during the remote X-ray diffraction data collections. We also thank the ChemCore from the Center for Molecular Innovation and Drug Discovery (CMIDD), Northwestern University for the help of inhibitor purity assays.

■ ABBREVIATIONS

NO, nitric oxide; NOS, nitric oxide synthase; nNOS, neuronal NOS; eNOS, endothelial NOS; iNOS, inducible NOS; $(Boc)_2O$, di-*tert*-butyl dicarbonate

■ REFERENCES

(1) Zhang, L.; Dawson, V. L.; Dawson, T. M. Role of Nitric Oxide in Parkinson's Disease. *Pharmacol. Ther.* **2006**, *109*, 33−41.

(2) Dorheim, M.-A.; Tracey, W. R.; Pollock, J. S.; Grammas, P. Nitric Oxide Synthase Activity Is Elevated in Brain Microvessels in Alzheimer's Disease. *Biochem. Biophys. Res. Commun.* **1994**, *205*, 659−665.

(3) Norris, P. J.; Waldvogel, H. J.; Faull, R. L. M.; Love, D. R.; Emson, P. C. Decreased Neuronal Nitric Oxide Synthase Messenger RNA and Somatostatin Messenger RNA in the Striatum of Huntington's Disease. *Neuronsicence* **1996**, *72*, 1037−1047.

(4) Ashina, M. Nitric Oxide Synthase Inhibitors for the Treatment of Chronic Tension-Type Headache. *Exp. Opin. Pharmacother.* **2002**, *3*, 395−399.

(5) Sims, N. R.; Anderson, M. F. Mitochondrial Contributions to Tissue Damage in Stroke. *Neurochem. Int.* **2002**, *40*, 511−526.

(6) Alderton, W. K.; Cooper, C. E.; Knowles, R. G. Nitric Oxide Synthases: Structure, Function and Inhibition. *Biochem. J.* **2001**, *357*, 593−615.

(7) Southan, G. J.; Szabó, C. Selective Pharmacological Inhibition of Distinct Nitric Oxide Synthase Isoforms. *Biochem. Pharmacol.* **1996**, *51*, 383−394.

(8) Babu, B. R.; Griffith, O. W. Design of Isoform-Selective Inhibitors of Nitric Oxide Synthase. *Curr. Opin. Chem. Biol.* **1998**, *2*, 491−500.

(9) Ji, H.; Erdal, E. P.; Litzinger, E. A.; Seo, J.; Zhu, Y.; Xue, F.; Fang, J.; Huang, J.; Silverman, R. B. In *Frontiers in Medicinal Chemistry*; Reitz, A. B., Choudhary, M. I., Atta-ur-Rahman, Eds.; Bentham Science Publishers: Oak Park, IL, 2009; Vol. *5*, pp 842−882.

(10) Hanessian, S.; Stoffman, E.; Mi, X.; Renton, P. Applications of Organocatalytic Asymmetric Synthesis to Drug Prototypes: Dual Action and Selective Inhibitors of *n*-Nitric Oxide Synthase with Activity Against the 5-$HT_{1D/1B}$ Subreceptors. *Org. Lett.* **2011**, *13*, 840−843.

(11) Ramnauth, J.; Speed, J.; Maddaford, S. P.; Dove, P.; Annedi, S. C.; Renton, P.; Rakhit, S.; Andrews, J.; Silverman, S.; Mladenova, G.; Zinghini, S.; Nair, S.; Catalano, C.; Lee, D. K. H.; De Felice, M.; Porreca, F. Design, Synthesis, and Biological Evaluation of 3,4-Dihydroquinolin-2(1*H*)-one and 1,2,3,4-Tetrahydroquinoline-Based Selective Human Neuronal Nitric Oxide Synthase (nNOS) Inhibitors. *J. Med. Chem.* **2011**, *54*, 5562−5575.

(12) Maddaford, S.; Annedi, S. C.; Ramnauth, J.; Rakhit, S. Advancements in the Development of Nitric Oxide Synthase Inhibitors. *Annu. Rep. Med. Chem.* **2009**, *44*, 27−50.

(13) Liang, G.; Neuenschwander, K.; Chen, X.; Wei, L.; Munson, R.; Francisco, G.; Scotese, A.; Shutske, G.; Black, M.; Sarhan, S.; Jiang, J.; Morizea, I.; Vaz, R. J. Structure-Based Design, Synthesis, and Profiling of Potent and Selective Neuronal Nitric Oxide Synthase (nNOS) Inhibitors with an Amidinothiophene Hydroxypiperidine Scaffold. *Med. Chem. Commun.* **2011**, *2*, 201−205.

(14) Silverman, R. B. Design of Selective Neuronal Nitric Oxide Synthase Inhibitors for the Prevention and Treatment of Neurodegenerative Diseases. *Acc. Chem. Res.* **2009**, *42*, 439−451.

(15) Ji, H.; Delker, S. L.; Li, H.; Martásek, P.; Roman, L. J.; Poulos, T. L.; Silverman, R. B. Exploration of the Active Site of Neuronal Nitric Oxide Synthase by the Design and Synthesis of Pyrrolidinomethyl 2-Aminopyridine Derivatives. *J. Med. Chem.* **2010**, *53*, 7804−7824.
(16) Xue, F.; Delker, S. L.; Li, H.; Fang, J.; Martásek, P.; Roman, L. J.; Poulos, T. P.; Silverman, R. B. Symmetrical Double-Headed Aminopyridines, a Novel Strategy for Potent and Membrane-Permeable Inhibitors of Neuronal Nitric Oxide Synthase. *J. Med. Chem.* **2011**, *54*, 2039−2048.
(17) Jing, Q.; Li, H.; Chreifi, G.; Roman, L. J.; Martásek, P.; Poulos, T. L.; Silverman, R. B. Chiral Linkers to Improve Selectivity of Double-Headed Neuronal Nitric Oxide Synthase Inhibitors. *Bioorg. Med. Chem. Lett.* **2013**, *23*, 5674−5679.
(18) Xue, F.; Gu, W.; Silverman, R. B. A Concise Route to the Chiral Pyrrolidine Core for Inhibitors of Neuronal Nitric Oxide Synthase. *Org. Lett.* **2009**, *11*, 5194−5197.
(19) Yuasa, Y.; Shibuya, S.; Yuasa, Y. The Oxidation of 3-Aryl-1-propenes by Oxidative System of $RuCl_3$-$NaIO_4$-Phase Transfer Catalyst. *Synth. Commun.* **2003**, *33*, 3947−3952.
(20) Poulos, T. P.; Li, H. Structural Basis for Isoform-Selective Inhibition in Nitric Oxide Synthase. *Acc. Chem. Res.* **2013**, *46*, 390−398.